Journal of Environmental Chemical Engineering 12 (2024) 112147

Contents lists available at ScienceDirect

Journal of Environmental Chemical Engineering

journal homepage: www.elsevier.com/locate/jece

Homogeneous vs. heterogeneous photo-Fenton elimination of antibiotic-resistant bacteria bearing intracellular or extracellular resistance: Do resistance mechanisms interfere with disinfection pathways?

Jeremie Decker [a,b], Truong-Thien Melvin Le [c], Jose Manuel Entenza [d,1], Isabel del Castillo Gonzalez [a], Aurelio Hernandez Lehmann [a], Cesar Pulgarin [c,e,f], Jorge Rodriguez-Chueca [b,*], Stefanos Giannakis [a,*]

[a] Universidad Politécnica de Madrid (UPM), E.T.S. de Ingenieros de Caminos, Canales y Puertos, Departamento de Ingeniería Civil: Hidráulica, Energía y Medio Ambiente, Unidad docente Ingeniería Sanitaria, c/ Profesor Aranguren, s/n, ES-28040 Madrid, Spain
[b] Universidad Politécnica de Madrid (UPM), E.T.S. de Ingenieros Industriales, Departamento de Ingeniería Química Industrial y del Medio Ambiente, c/ José Gutiérrez Abascal 2, Madrid 28006, Spain
[c] School of Basic Sciences (SB), Institute of Chemical Science and Engineering (ISIC), Group of Advanced Oxidation Processes (GPAO), École Polytechnique Fédérale de Lausanne (EPFL), Station 6, CH-1015 Lausanne, Switzerland
[d] Faculty of Biology and Medicine, Department of Fundamental Microbiology, University of Lausanne (UNIL), Biophore Building, CH-1015 Lausanne, Switzerland
[e] Colombian Academy of Exact, Physical and Natural Sciences, Carrera 28 A No. 39A-63, Bogotá, Colombia
[f] Environmental Remediation and Biocatalysis Group, Institute of Chemistry, Faculty of Exact and Natural Sciences, University of Antioquia, Calle 70 No. 52–21, Medellín, Colombia

ARTICLE INFO

Editor: Luigi Rizzo

Keywords:
Antibiotic resistance genes
Antibiotic tolerance
Disinfection
Photo-Fenton process
Staphylococcus aureus

ABSTRACT

The present study aimed to fill the knowledge gap between the implications of intracellular and extracellular antibiotic resistance mechanisms may inflict on the inactivation pathways of the photo-Fenton process under mild conditions. It was thus designed as a cross-comparison of the effect of homogeneous and heterogeneous photo-Fenton (near-neutral pH, [Fe]=1 mg/L, and [H_2O_2]=10 mg/L) on seven strains of *Staphylococcus aureus* exhibiting different mechanisms of antibiotic resistance, or susceptibility. Additionally, variations in antibiotic tolerance (MIC test) and relative changes in the presence of antibiotic resistance genes were qualitatively monitored during treatment using PCR. The results suggest that resistance to antibiotics does not confer enhanced resistance to photo-Fenton, as it attained a 4-logU reduction within 50–100 min for all strains, regardless of resistance status. Strains that express intracellular resistance mechanisms do not pose a risk; however, strains that express external mechanisms for their defense against antibiotics occasionally interfere with the inactivation process. This phenomenon was mainly linked to the cell wall thickening of some of the externally resistant strains as compared to their susceptible homologues. Eventually, by conferring resistance to antibiotics, this cell wall alteration may reduce susceptibility to Fenton-related reagents by either reducing their intracellular diffusion or rendering cell walls less prone to leaching upon extracellular attacks. In addition, the photo-Fenton process either remained unchanged or lowered the antibiotic resistance threshold. Moreover, the homogeneous photo-Fenton system considerably lowered the detection of antibiotic resistance genes within 90 min with respect to *hv*, *hv*/H_2O_2, or heterogeneous photo-Fenton. In conclusion, the results suggest that the homogeneous photo-Fenton system could be an effective treatment for hindering the spread of antibiotic resistance, but treatment conditions should aim to maximize the degradation of ARG, as their concentration decreases more slowly than that of bacteria.

Abbreviations: AB, antibiotics; ABR, antibiotic resistance; ARB, antibiotic-resistant bacteria; ARG, antibiotic-resistant genes; CIP, Ciprofloxacin; VAN, Vancomycin; *hv*, solar light; FeOx, iron oxide; PF-Fe^{2+}, homogeneous photo-Fenton process; PF-FeOx, heterogeneous photo-Fenton process (with natural iron oxides).

* Corresponding authors.
E-mail addresses: jorge.rodriguez.chueca@upm.es (J. Rodriguez-Chueca), stefanos.giannakis@upm.es (S. Giannakis).

[1] The author Prof. Dr. J. Entenza, of the University of Lausanne, has passed away.

https://doi.org/10.1016/j.jece.2024.112147
Received 24 November 2023; Received in revised form 30 January 2024; Accepted 3 February 2024
Available online 6 February 2024

1. Introduction

Antibiotics (AB) remain the major discovery of modern medicine and are currently the treatment of choice for bacterial infection-related diseases [1]. However, over the past few years, their effectiveness has been threatened because bacteria express novel genes conferring resistance properties, effectively converting them into antibiotic-resistant bacteria (ARB) [2,3]. Within this context, the horizontal transmission of genes that confer resistance to antibiotics (antibiotic resistance genes, hereon: ARG) has been highlighted as a major concern in the ongoing combat against ABR [4], as susceptible bacteria can inherit these resistance properties from other live or inactivated cells, rendering them resistant to AB.

With regard to the phenotype, the transcription of these genes manifests through specific mechanisms, which can be classified into four categories: i) the production of anti-drug compounds, such as beta-lactamases, ii) the reduction of AB penetration into the bacterial cell by downregulation of protein channels (porins), iii) the active removal of intracellular AB by the expression of efflux pumps, and iv) the alteration of binding sites located on the bacterial wall serving as entry pathways for AB [5]. Generally, intracellular and/or extracellular mechanisms can be deployed to protect cells from AB. It is not uncommon for bacteria to develop more than one mechanism, corresponding to multiple drug protection, denominated as multidrug-resistant (MDR) bacteria.

It is estimated that by 2050, the number of deaths related to antibiotic-resistant infections worldwide will increase to 10 million per year [6]. This rising concern urges the development of novel antimicrobial treatments, as well as the implementation of technical strategies to curb the acquisition of resistance among bacteria. The One Health Initiative aims to address the latter by simultaneously acting on the health of humans, animals, and the environment. In principle, actions should be taken by implementing policies to reduce the overuse and disposal of AB, planning surveillance and monitoring, and developing therapeutic alternatives to combat bacteria in medical settings such as hospitals, veterinary settings, and farms [7]. Additionally, the reduction of AB and ARB disposal into the environment is desirable, notably through the improvement of processes used for the treatment of municipal wastewater (MWW). It is estimated that the disposal of WW is one of the major vectors for the dissemination of ABR [8]. Most wastewater treatment plants (WWTPs) are currently underequipped to meet the current challenges and usually lack oxidative treatment steps [9]. Recalcitrant compounds such as AB are thus only partially degraded, and their disposal into the environment eventually pressures bacteria towards the acquisition of resistance [10]. Additionally, bacterial disinfection has been shown to leach intact genetic material. In ARB, leaching of ARG and its disposal into the environment is an ideal pathway for resistance acquisition through horizontal gene transfer by antibiotic-susceptible bacteria [11].

Oxidative treatments have been extensively investigated to address the decontamination of wastewater by both ARB and ARG. Recently, promising results have been achieved at bench- and pilot-scales using ozonation, chlorination, light/H_2O_2, homogenous photo-Fenton, and heterogeneous TiO_2 catalysts [12]. Despite these encouraging results, it is still important to deepen our understanding of resistance mechanisms and, specifically, how they affect the effectiveness of bacterial inactivation through photochemically produced reactive intermediates (PPRIs) generated upon AOPs.

Although the photo-Fenton process is now widely known for its effectiveness in disinfecting contaminated water at the bench scale [13–15] and, more recently, at the field scale [16], its effectiveness within the context of ABR has consistently been shown to be inferior to other conventional disinfection processes such as ozonation and chlorination [17] or UV-C-based processes [18]. Nonetheless, the photo-Fenton process should not be discredited as a viable alternative to conventional processes, especially because of its end-application advantages, such as its economic feasibility [19] and reduced toxicity in the efflux stream [20]. Moreover, recent studies have shown that the acquisition of AB resistance does not alter the susceptibility to the photo-Fenton [21,22]. This conclusion was also drawn at the field scale using municipal wastewater [23]. Complementarily, the photo-Fenton process has also demonstrated satisfactory ARG removal potential [24,25]. In this context, further studies to elucidate the disinfection pathways of resistant strains are necessary to guide the effective application of the photo-Fenton process, as effective engineering implementation of the process could palliate its lower efficacy compared to conventional disinfection processes.

Thus, we would like to stress the necessity of a thorough investigation of how distinct steps of the Fenton reaction could be affected by the different modes of action of antibiotic resistance. Specifically, as bacteria may develop diverse strategies of resistance, the present work is an attempt to discriminate between these two categories of resistance, namely extra- or intracellular, and to establish how these would affect the effectiveness of the intracellular or extracellular photo-Fenton process. Hereafter, the internal photo-Fenton process refers to the set of intracellular damages caused by intracellular PPRIs via the Fenton reaction, whereas the external photo-Fenton process refers to the extracellular damage caused by extracellularly generated PPRIs via the Fenton reaction and the direct action of iron-containing species on the cell wall.

The homogeneous and heterogeneous photo-Fenton processes have distinct inactivation mechanisms. In the first case, because H_2O_2 and Fe^{2+} are present both intra- and extracellularly and can diffuse through the bacterial wall, the generated radicals (Scheme 1, R.1–3) simultaneously attack the bacterial membrane and intracellular biological materials (DNA, lipids, and proteins). Additionally, ferric ions can be reduced through Ligand-to-Metal Charge Transfer (LMCT) causing additional damage to the bacterial wall (R.4). Under heterogeneous conditions, only H_2O_2 diffuses inside the cell. Consequently, the radicals generated by iron oxides (R.5–6) primarily attack the outer membrane of the cell. The cell wall can also be directly damaged by LMCT (R.7) [26].

As shown in Scheme 1, light inhibits the activity of enzymes responsible for the scavenging of intracellular hydrogen peroxide while favoring the release of ferrous ions from iron-containing proteins. This phenomenon favors an increased concentration of Fenton reagents inside the bacterial cell, permitting intracellular photo-Fenton reactions to occur [27]. This internal bactericidal pathway is favored by the diffusion of reagents under homogeneous conditions [28], but remains secondary under heterogeneous conditions [29].

Based on these distinctions, this study was designed to compare the sensitivities to either external or internal photo-Fenton of several strains of *Staphylococcus aureus*, both antibiotic-susceptible and antibiotic-resistant, bearing either external or internal resistance. In our study, disinfection by solar light (*hν*), hydrogen peroxide under solar light (*hν*/H_2O_2), homogeneous photo-Fenton mediated by iron salts under solar light (hereafter, PF-Fe^{2+}), and heterogeneous photo-Fenton mediated by iron oxides (hematite) under solar light (hereafter, PF-FeOx) were investigated. These processes were applied to the following strains: two methicillin-susceptible *S. aureus* (MSSA) strains and their isogenic ciprofloxacin-resistant strains (MSSA1112, MSSA133, MSSA1112-CipR, and MSSA133-CipR), as well as methicillin-resistant *S. aureus* (MRSA) and its isogenic vancomycin-resistant strains, MRSA VISA PC-1, MRSA VISA PC-3 * , and MRSA VISA 1050. Finally, these were also applied to the *Escherichia coli* strain containing the identified model ARG, namely $bla_{CTX\text{-}M\text{-}9}$, to monitor the corresponding ARG degradation, and a wild-type *E. coli* K12 strain was used for complementary and validation tests as this strain was from a collection and is particularly well documented.

This experimental design aimed to determine whether resistance to AB alters the sensitivity of bacteria to photo-Fenton processes under ideal laboratory conditions. In this case, it should be determined

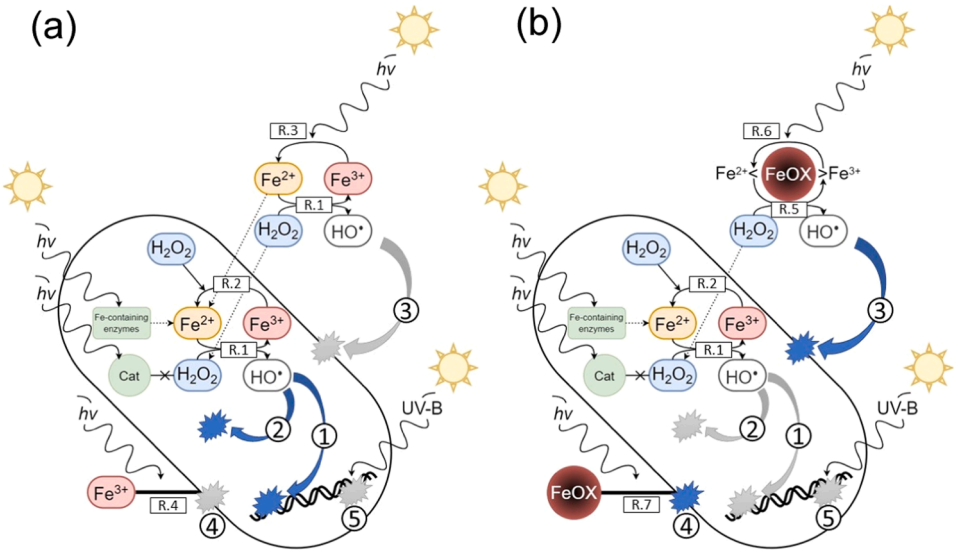

Scheme 1. a) Bactericidal mechanism of action of heterogeneous photo-Fenton reaction: Internal Fenton attacks DNA (1), proteins, and lipids (2). The external Fenton (3) and LMCT (4) processes damage the external membrane. Mutagenic UV-B directly attacks the DNA (5). In homogeneous conditions, the main driver is the internal Fenton reaction (blue), which is favored by the diffusion of reagents. b) The pathways are similar under heterogeneous conditions; however, the main driver is external attacks (blue), as the iron source is diffusion-limited. Reactions "R.X" are detailed in the main text.

whether the reduced sensitivity differs depending on the type of AB resistance and/or the Fenton mode of action (i.e., extra- or intracellular Fenton). Analogically, the way different Fenton modes of action would degrade intracellular ARG, and how the treatment could modify AB tolerance among surviving bacterial populations should also be assessed. We expect the results to support and help direct ongoing research for the effective treatment of real wastewater using the (photo-) Fenton process.

2. Materials and methods

2.1. Chemicals and reagents

Hydrogen peroxide (H_2O_2, CAS 7722–84-1) 30% (w/w) was used for the processes of solar-H_2O_2 ($h\nu/H_2O_2$), of solar photo-Fenton (PF-Fe^{2+}) and heterogeneous solar photo-Fenton (PF-FeOx) processes. $FeSO_4{\cdot}7\ H_2O$ (CAS 7782–63-0) was used in the process of PF-Fe^{2+}. Ti(IV) oxysulfate ($TiOSO_4$, CAS 13825–74-6) 1.9–2.1% was used to quantify the hydrogen peroxide. All of the above-mentioned compounds were purchased from Sigma-Aldrich (Buchs, Switzerland). The iron oxides used for PF-FeOx were extracted from an iron mine in Colombia (Duitama, Boyacá). These oxides were characterized in a previous study [30] and were shown to have an iron content of 81.26% (α-Fe_2O_3) and a specific surface area of 19.79 m^2/g (Brunauer-Emmett-Teller theory).

Bacteria were cultivated in Tryptic Soy Agar (TSA), Tryptic Soy Broth (TSB), and Brain Heart Infusion Agar (BHIA) from BD Biosciences (Franklin Lakes, NJ, USA). ETEST® strips were purchased from Biomérieux (Lyon, France) and were used to determine the Minimal Inhibitory Concentration (MIC) of both ciprofloxacin and vancomycin.

Primers used for PCR were acquired from Microsynth (Switzerland). Agarose and 1 kb DNA Ladder used for electrophoresis were purchased from Promega (Dübendorf, Switzerland), and SYBR safe DNA gel stain was purchased from Invitrogen (Basel, Switzerland).

2.2. Bacterial strains

The present study used seven strains of *Staphylococcus aureus* and two *E. coli* strains. *S. aureus* strains were susceptible or resistant to either ciprofloxacin or vancomycin, whereas *E. coli* strains were either AB susceptible or resistant to β-lactam. The strains were maintained as follows: bacteria were stored at − 80 °C in TSB containing 10% (v/v) glycerol. The stock was prepared by growing bacteria on TSA plates overnight. The plates were stored at 4 °C. One colony was inoculated into TSB and incubated overnight at 37 °C. Bacteria were washed twice with phosphate buffer solution (PBS) prior to use and dispersed in water to achieve working concentrations of 10^6 CFU/mL.

The strains used in the present study are listed in Table 1. From MSSA 1112 and 133, the isogenic ciprofloxacin-resistant homologues MSSA 1112-CipR and MSSA 133-CipR were isolated after the development of resistance. Briefly, MSSA 1112 and MSSA 133 strains were subcultured

Table 1
Bacterial strains used in the study, their resistance, and references.

Strain	Resistance	Genotype	Reference/ source
MSSA 1112	-	Wild type, not antibiotic resistant	[32]
MSSA 133	-	Wild type, not antibiotic resistant	[33]
MSSA 1112-CipR	CIP	As MSSA 1112; CIP resistant homologue, isolated after CIP development (in vitro)	This study
MSSA 133-CipR	CIP	As MSSA 133; CIP resistant homologue, isolated after CIP development (in vitro)	This study
MRSA PC-1	Methicillin	Wild type, clinical isolate	[31]
VISA PC-3 *	Methicillin and VAN	As MRSA PC-1 with VAN resistance development in vivo (named PC-3) and VAN-resistant (*van*A) derivative of clinical isolate PC-3 (in vitro)	[31]
VISA 1050	Methicillin and VAN	As MRSA PC-1; isogenic homologue, VAN-resistant (*van*A) derivative of clinical isolate PC-1 (in vitro)	This study
***E. coli* K-12 (DSM 498)**	-	Wild type, collection sourced	[34]
***E. coli* ESBL 8543**	β-lactam producing, Cefotaxime resistant	$bla_{CTX\text{-}M}$	[35]

on CIP-enriched media. Subcultures served as bacterial stocks for MSSA 1112-cipR and MSSA 133-cipR strains.

The methicillin-resistant *S. aureus* (MRSA) strain VISA PC-1 is susceptible to vancomycin (MIC=2 μg/mL) [31]. More details regarding the strain isolation can be found in the Supplementary Information. Similar to the development of CIP resistance, the procedure described above was used to develop the resistant strain VISA 1050 from MRSA PC-1 in VAN-enriched media. Complementary tests were performed on well-documented culture-sourced *E. coli* K-12 obtained from the German Collection of Microorganisms and Cell Cultures (DSMZ).

2.3. Experimental apparatus and methods

Experiments were conducted in Pyrex Erlenmeyer flasks mounted with a screw cap. These were mechanically stirred and placed in a Heraus SUNTEST CPS Solar Simulator under an irradiance of 750 W/m^2 (emitted by a 1500-W xenon lamp). This fixed irradiance was chosen because it permits proper kinetics monitoring; this value is sufficiently high for the photo-Fenton process to exhibit a measurable effect, but is not the main driving force of bacterial inactivation [36]. The 750 W/m^2 value corresponds to a moderate level for the Mediterranean basin (yearly average), for which previous solar-only disinfection experiments showed that 4-logU *E. coli* inactivation could be achieved, accounting for the prevailing meteorological conditions [37,38]; hence, the photo-Fenton process could also be successfully implemented.

All reactors were filled with 40 mL of ultrapure water spiked with bacteria at a final concentration of 10^6 CFU/mL and exposed to light. Four reactors were placed symmetrically on 15-slot stirrers to ensure homogeneous exposure to light and mixed with the inserted magnetic bars. Blank experiments without light were performed in amber reactors and wrapped with aluminum foil to ensure that these tests, except for the light supply, were otherwise identical. Additionally, chemical reagents were added accordingly to reach the following final concentrations: for *hν*/H_2O_2, 10 mg/L of hydrogen peroxide; for PF-Fe^{2+}, 10 mg/L of hydrogen peroxide and 1 mg/L of Fe^{2+} from $FeSO_4{\cdot}7\ H_2O$; and for PF-FeOx, 10 mg/L of hydrogen peroxide and 1 mg/L of total iron. During the experiment, 1-mL samples were periodically collected and neutralized with catalase (200 U/mL). These were used for either qualitative ARG determination (detailed below) or bacterial cultivability monitoring. Scheme 2 represents the experimental setup of the study, including the solar simulator, together with basic information on the preparation of samples, stirrers, reactors, and experimental conditions (temperature, irradiance, and reagent concentration).

For bacterial counts, 10-fold serial dilutions were prepared, plated on BHIA, and incubated overnight. The number of colonies was adjusted based on the number of dilutions and standardized to the initial concentration (10^6 CFU/mL). For simplicity, blank tests (non-treated samples) were not plotted; all strains were stable in the dark for the entire duration of the experiment. The inactivation curve was fitted using the GInaFit add-on in Excel [39]. Fitting was performed using either the shoulder-log linear decay model or the shoulder plus shoulder-log linear decay model [40]. Additionally, the concentration of hydrogen peroxide was monitored by colorimetry using $TiOSO_4$ (DIN 38 402 H15). Briefly, 1 mL of a filtered sample (0.45 μm PTFE filters) was mixed with 20 μL of $TiOSO_4$ solution, and the absorbance was measured by spectrophotometry (UV-1800, Shimadzu) at 410 nm. All experiments were conducted in triplicate, and the points in the graphs represent average values and standard deviations.

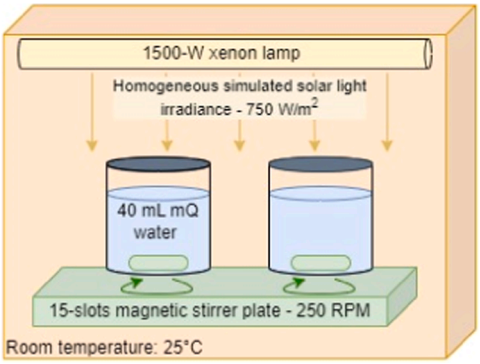

Scheme 2. – Experimental setup for disinfection experiments in a sun simulator. Symmetrically placed 40-mL reactors (blue) were constantly irradiated by homogeneous simulated solar light (yellow) inside the solar simulator (orange). Agitation was ensured by placing magnetic bars (green) inside the reactor and stirring with a magnetic plate at a rate of 250 RPM.

2.4. Determination of antibiotic susceptibility

For the evolution of antibiotic susceptibility, samples were collected for cultivability testing and, in parallel, their minimal inhibitory concentrations (MIC) were determined using ETEST® strips. A colony was inoculated into tryptic soy broth (TSB) and grown overnight at 37 °C. The bacteria were washed twice, diluted 100-fold, and spread on Brain Heart Infusion Agar (BHIA)-containing plates. An ETEST® strip was placed directly on the agar surface. The plates were incubated overnight at 37 °C and the MIC was determined visually.

2.5. Determination of concentration of model ARG

The evolution of $bla_{CTX\text{-}M\text{-}9}$ gene in the model organism was assessed by polymerase chain reaction (PCR). The bacteria from the samples were lysed, and ARG evolution was monitored following a previously described method for $bla_{CTX\text{-}M\text{-}9}$ determination [41]. $bla_{CTX\text{-}M\text{-}9}$ degradation was qualitatively assessed by migration on an agarose gel. The primers used are listed in Table 2.

2.6. Experimental design

The present study was conceptualized as a cross-sectional comparison between extra- or intracellular oxidative processes and extra- or intracellular antibiotic resistance mechanisms. The experimental plan was laid out to assess the following five hypotheses and research questions:

(i) Does acquired antibiotic resistance alter the sensitivity of bacterial strains to oxidative processes?
(ii) Do distinct mechanisms of resistance confer different sensitivities to oxidative processes?
(iii) Does the mode of action of the disinfection process (extracellular or intracellular) play a key role in the efficacy of disinfection with respect to the resistance mechanism of AB?
(iv) In the case of bacterial survival, is the antibiotic tolerance threshold modified?
(v) How differently does the mode of action (extracellular or intracellular) of the process degrade antibiotic resistance genes (ARG)?

In the first part, we addressed hypotheses (i)–(iii) by comparing the disinfection curves of two strains exhibiting an intracellular mechanism of resistance to the disinfection curves of two strains exhibiting an extracellular mechanism of resistance. Disinfection experiments were conducted as detailed in Section 2.3. Strain selection was performed based on the following considerations: *Staphylococcus aureus* was chosen for its sanitary relevance, as well as for its extensively studied mechanisms of antibiotic resistance. The discrimination between intra- and extracellular modes of antibiotic resistance was based on the development of resistance ciprofloxacin (CIP) and vancomycin (VAN). The discrimination was based on the detailed differences presented below.

CIP is a fluoroquinolone that has been extensively used to treat a

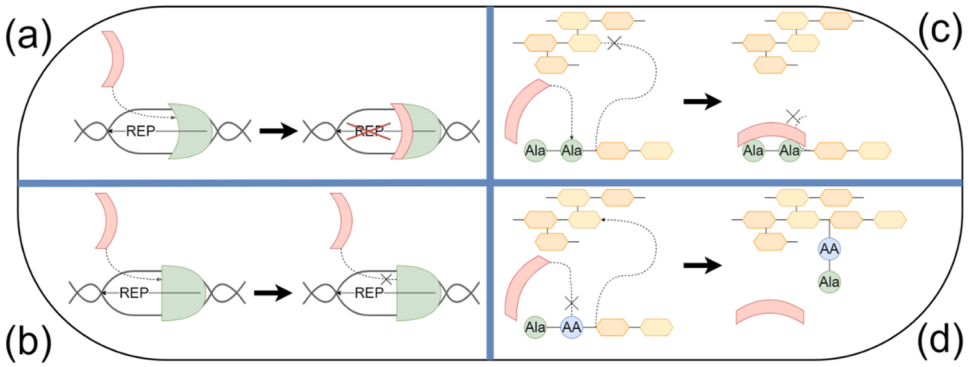

Scheme 3. a) mode of action of CIP by prevention of the DNA replication. b) mechanism of resistance to CIP by alteration of the target enzyme topoisomerase IV. c) mode of action of VAN, by prevention of the cell wall polymerization. d) mechanism of resistance to VAN by alteration of the targeted amino acids sequence (AA: altered amino acid).

Table 2
Primers for the PCR of the bla$_{CTX\text{-}M\text{-}9}$ ARG.

Gene	Direction	Primers sequences (5´→3´)	Product size [bp]
bla$_{CTX\text{-}M\text{-}9}$	Forward	ATGGTTAAAAAATCACTGCGCCAG	869
	Reverse	CCGTCGGTGACGATTTTAGCCG	

wide range of infections [42]. It inhibits enzymatic activity involved in DNA decatenation [43]. Specifically for the case of *Staphylococcus aureus*, CIP was found to bind with the enzyme topoisomerase IV. The stable enzyme-DNA-quinolone complex blocks DNA replication, eventually leading to cell lysis [44]. Genomic mutations have been highlighted in *grlA* and *grlB*, which encode subunits A and B of topoisomerase IV, respectively [45]. The mutated amino acid sequence in the quinolone-resistance-determining region of the enzyme reduces its affinity for CIP while preserving its decatenation activity.

VAN is a glycopeptide antibiotic used extensively to treat patients infected with methicillin-resistant *Staphylococcus aureus* (MRSA) [46]. Briefly, the cell wall is composed of rigid polymer layers [47]. During cell wall synthesis, D-Ala-D-Ala-terminated murein monomers were integrated into the polymers [48]. VAN inhibits synthesis by preventing polymerization of the above-mentioned monomers [49,50]. Several mechanisms of VAN resistance have been identified: (i) thickening of the cell wall prevents the mobility of AB [51]; (ii) the expression of false targets prevents VAN from accessing the site of wall synthesis [52]; and (iii) modification of the residue D-Ala-D-Ala into other amino acids hinders the binding of VAN [53,54].

In the second part, hypothesis (iv) was addressed by comparing the MIC (determined using ETEST® strips) of each antibiotic-resistant bacterial strain pre- and post-treatment via an oxidative process. Finally, hypothesis (v) was addressed by qualitatively comparing the relative degradation of the model ARG *bla$_{CTX\text{-}M\text{-}9}$* among the various treatment methods. The *E. coli* ESBL 8543 strain containing *bla$_{CTX\text{-}M\text{-}9}$* was exposed to external and internal oxidative processes, and gene detection was monitored during the experiment.

3. Results

3.1. Disinfection of S. aureus deploying internal antibiotic resistance mechanisms

Homogeneous and heterogeneous photo-Fenton processes were applied stepwise to the model strains for the internal mechanism of resistance to antibiotics, namely, CipR MSSA 1112 and MSSA 133. Figs. 1(a) and 1(b) show the two antibiotic-susceptible (ABS) strains used as controls in blue and the two antibiotic-resistant (ABR) strains in red. First, light alone was capable of disinfecting *S. aureus*, whereas the

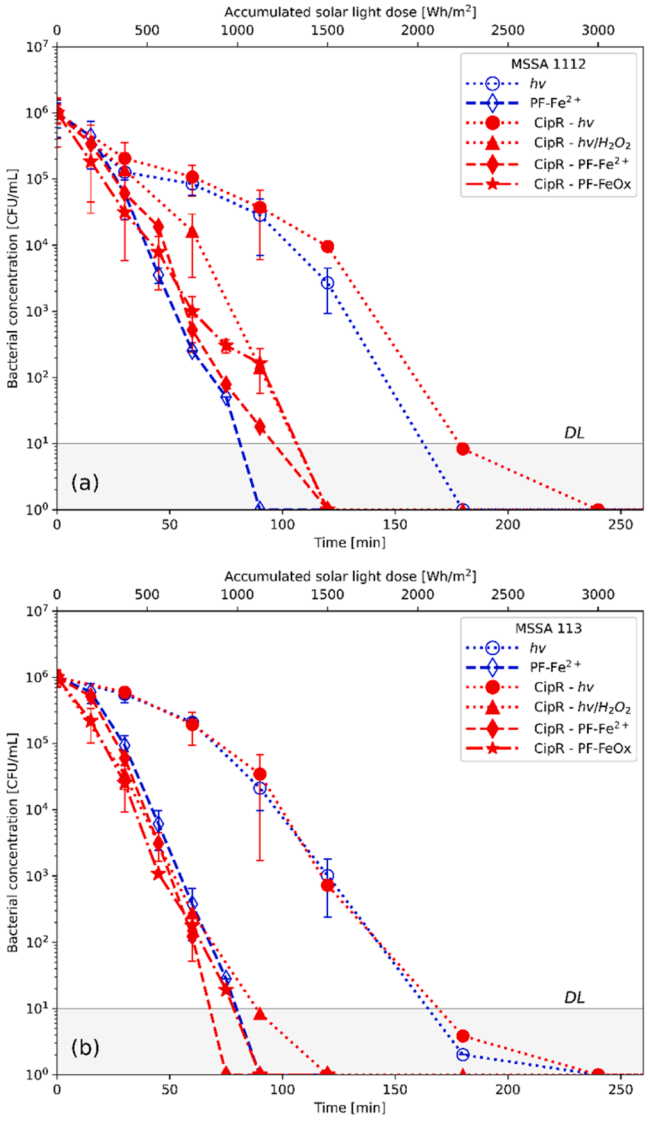

Fig. 1. Disinfection profiles of ciprofloxacin-resistant S. aureus strains under solar light (hv), solar light and hydrogen peroxide hv/H_2O_2, homogeneous solar photo-Fenton PF-Fe^{2+} and heterogeneous solar photo-Fenton PF-FeOx. The strains used were: a) MSSA 1112 CipR (plain, red) and isogenic ABS strain MSSA 1112 as control (unfilled, blue); and b) MSSA 133 CipR (plain, red) and isogenic ABS strain MSSA 133 as control (unfilled, blue). Experimental conditions: I = 750 W/m^2, [Fe] = 1 mg/L, [H_2O_2] = 10 mg/L. DL: Detection limit.

addition of H_2O_2 enhanced inactivation kinetics. The addition of iron (in any form) resulted in an additional increase in the first phase of the reaction; however, the process seemed to be governed by H_2O_2-mediated inactivation.

Regarding the two types of *S. aureus*, we reported that the susceptible strains did not differ significantly from their resistant counterparts. Specifically, MSSA 1112 showed differences within the margin of error under plain solar exposure and PF-Fe^{2+}, whereas no difference was observed for MSSA 133. Comparing the two modes of the PF process (see Table S1), the disinfection of the resistant strain showed no difference when compared to the isogenic susceptible strain, and the kinetics of PF-Fe^{2+} compared to PF-FeOx for the resistant strains were quasi-similar.

Additionally, to discriminate the mode of action of both PF-Fe^{2+} and PF-FeOx (intra- and extracellular, respectively), a complementary experiment was performed using a typical $HO^{\bullet}$ scavenger, tert-butanol (TBA) (6×10^8 $M^{-1}s^{-1}$) [55]. This scavenger assay was performed on *E. coli* K-12, an extensively well-documented collection strain of *E. coli* (Table 1, Section 2.2) for better comparability, in which both processes were applied in the presence or absence of the scavenger. By doing so, as shown in Table 3, the rate of inactivation was particularly affected in the case of PF-FeOx (71.4% decrease in the apparent reaction rate without TBA) compared with only 23.5% in the case of PF-Fe^{2+}. This result supports the difference between the two processes, where external attacks by exogenous $HO^{\bullet}$, which drives the PF-FeOx process, are slowed down because of their competition with TBA, to a greater extent than PF-Fe^{2+}.

3.2. Comparison of disinfection processes against isogenic methicillin-resistant S. aureus (MRSA) exhibiting extracellular resistance

Homogeneous and heterogeneous photo-Fenton processes were applied stepwise to the model strains for external mechanisms of resistance to antibiotics, namely, VISA PC-3 * and VISA 1050. Figs. 2(a) and 2(b) show the two ABS strains used as controls in blue and the two ABR strains in red. As opposed to the internal resistance mechanism, some differences are worth mentioning.

First, while the baseline solar inactivation did not differ between the susceptible and resistant isogenic MRSA PC-1 and VISA PC-3 * strains, the resistant VISA 1050 strain was found to have a prolonged lag period (shoulder length of 30 min) compared to the susceptible strain (both values can be found in the kinetic analysis presented in Table S2 of Supplementary Information). However, the rate increased sharply, resulting in a similar time for 4-log disinfection (Table 4). The addition of H_2O_2, similar to MSSA 1112 and 133, reduced the time required to reach total inactivation for both the PC-3 * and 1050 strains. Besides, the addition of ferrous iron resulted in a higher inactivation effect only for VISA PC-3 * , and the VISA 1050 strain exhibited identical kinetics regardless of the presence or absence of iron.

Concerning the PF modes, it appears that the PF-Fe^{2+} process inactivates both resistant strains at different rates. In fact, in comparison to their susceptible homologues, the inactivation of VISA PC-3 * was faster and without a lag phase; it was inactivated at a high initial rate, which decreased around 30–45 min. This phenomenon appeared to have a tailing effect on the inactivation curve. In contrast, PF-Fe^{2+}-mediated inactivation was slower in VISA 1050. This strain is credited to having a thicker cell wall and may have manifested delayed inactivation because of the reduction in the intracellular diffusion rate of the Fenton reagents.

Table 3
Variation in apparent first-order reaction rate constant of disinfection of wild-type E. coli K12 for both processes in the presence or absence of $HO^{\bullet}$ scavenger ($[TBA]_o = 10$ mM).

Process	No scavenger	Scavenger
PF-Fe^{2+}	100%	76.4%
PF-FeOx	100%	28.6%

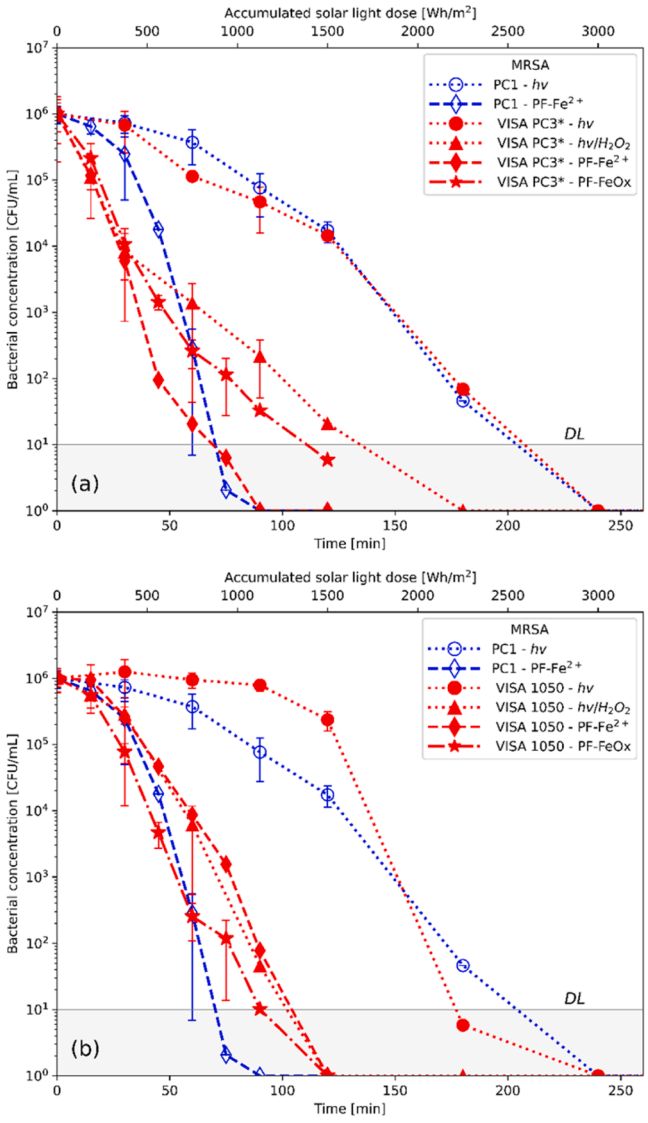

Fig. 2. Disinfection profiles of vancomycin-resistant S. aureus strains under solar light (hv), solar light and hydrogen peroxide hv/H_2O_2, homogeneous solar photo-Fenton PF-Fe^{2+} and heterogeneous solar photo-Fenton PF-FeOx. The strains used were: a) VISA PC-3 * (plain, red) and isogenic ABS strain PC-1 as controls (unfilled, blue); b) VISA 1050 (plain, red) and isogenic ABS strain PC-1 as controls (unfilled, blue). Experimental conditions: I = 750 W/m^2, [Fe] = 1 mg/L, [H_2O_2] = 10 mg/L. DL: Detection limit.

This consideration remains relevant, as it has previously been shown that staphylococcal strains are sensitive to cell surface damage in a heterogeneous system in another study [56], in which the authors confirmed by SEM imaging that the presence of iron-based composites, hydrogen peroxide, and irradiation caused noticeable cell surface damage. In our case, PF-FeOx yielded the fastest inactivation of VISA 1050 because the inhibited diffusion rate did not damage the cell wall. However, it inactivated PC-3 * slower than PF-Fe^{2+}, as the formation of particle-bacteria and bacteria-bacteria aggregates reduced the contact surface between the cell wall and FeOx, thus decreasing the inactivation potential.

3.3. Alteration of antibiotic susceptibility by treatment: MIC tests

Table 5 shows the variations in antibiotic susceptibility post-treatment. For MSSA 1112 CipR, the MIC was not modified post-treatment for any of the *hv*, *hv*/H_2O_2, PF-Fe^{2+}, or PF-FeOx processes.

Table 4
Time values (min) for 4-logU reduction of CFU bacterial concentrations by all four processes, namely solar light (hv), solar light and hydrogen peroxide (hv/H_2O_2), homogeneous solar photo-Fenton ($PF\text{-}Fe^{2+}$), and heterogeneous solar photo-Fenton (PF-FeOx) for susceptible and resistant strains, as obtained by fitting the log-linear model with a delay period.

	Strain	*hv* only	hv/H_2O_2	$PF\text{-}Fe^{2+}$ (intracellular)	PF-FeOx (extracellular)
ABS	MSSA 1112	±156.6 min	-	±66.6 min	-
	MSSA 133	±156 min	-	±67.5 min	-
Internal ABR	MSSA 1112 CipR	±180 min	±96 min	±79.2 min	±85.2 min
	MSSA 133 CipR	±158.4 min	±74.4 min	±59.3 min	±63 min
ABS	VISA PC1	±182.4 min	-	±66.6 min	-
External ABR	VISA PC-3*	±182.4 min	±99 min	±50.4 min	±75.6 min
	VISA 1050	±180 min	±88.8 min	±90 min	±75.6 min

Table 5
MIC evolution of ABR post-treatment, with the initial and final MIC values (μg/mL) and treatment duration (min).

	Strain	*hv* only	hv/H_2O_2	$PF\text{-}Fe^{2+}$ (intracellular)	PF-FeOx (extracellular)
Internal Resistance	MSSA 1112 CipR	= **(>32 μg/mL)** (120 min)	= **(>32 μg/mL)** (60 min)	= **(>32 μg/mL)** (60 min)	= **(>32 μg/mL)** (90 min)
	MSSA 133 CipR	↑ **(12 to >32 μg/mL)** (120 min)	↓ **(>32 to 12 μg/mL)** (60 min)	= **(12 μg/mL)** (60 min)	= **(>32 μg/mL)** (60 min)
External Resistance	VISA PC-3 *	↑ **(6 to 8 μg/mL)** (120 min)	= **(8 μg/mL)** (90 min)	↓ **(8-12 to 8 μg/mL)** (30 min)	= **(8 μg/mL)** (60 min)
	VISA 1050	↑ **(1-2 to 2 μg/mL)** (120 min)	= **(2 μg/mL)** (60 min)	↓ **(3 to 1 μg/mL)** (90 min)	= **(3 μg/mL)** (45 min)

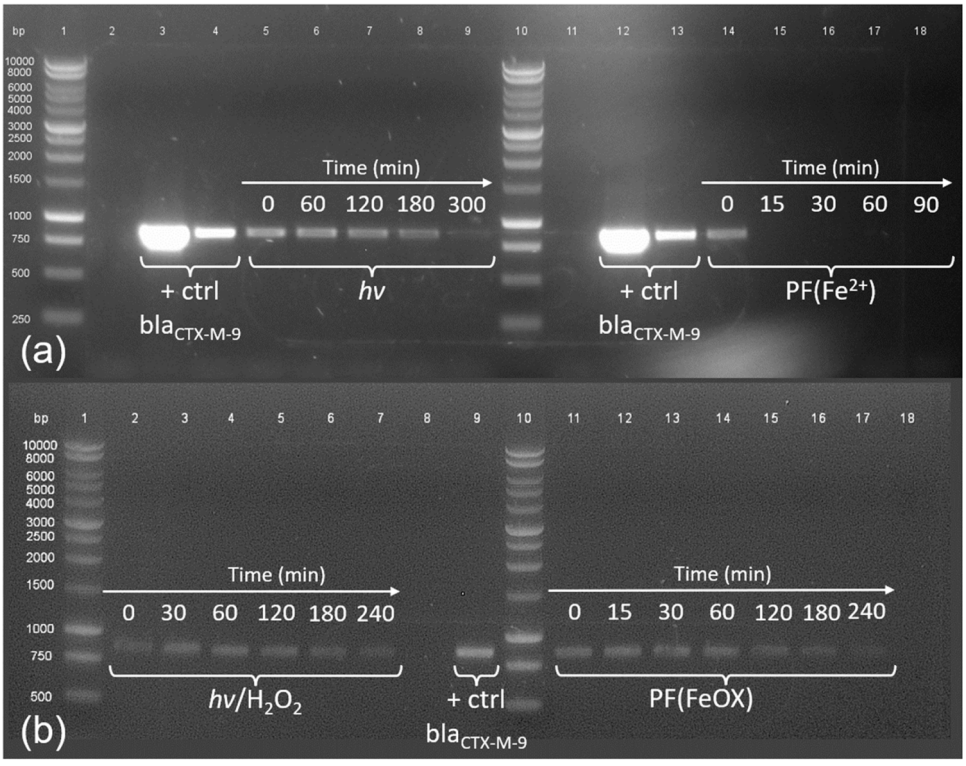

Fig. 3. Gel electrophoresis of PCR products targeting $bla_{CTX\text{-}M\text{-}9}$ in E. coli ESBL 8543. (a) Lanes 1 and 10:1 kb DNA ladder; lanes 2 and 11: negative PCR control; lanes 3 and 12: $bla_{CTX\text{-}M\text{-}9}$ positive control; lanes 4 and 13: positive control diluted 100x; Lanes 5 to 9: samples taken after 0, 60, 120, 180, and 300 min of hv treatment; lanes 14 to 18: samples taken after 0, 15, 30, 60, and 90 min of $PF\text{-}Fe^{2+}$ treatment. (b) Lanes 1 and 10:1 kb DNA ladder; lane 8: negative PCR control; lane 9: $bla_{CTX\text{-}M\text{-}9}$ positive control diluted 100x; Lanes 2–7: samples taken after 0, 30, 60, 120, 180, and 240 min of solar hv/H_2O_2 treatment; lanes 11–17: samples taken after 0, 15, 30, 60, 120, 180, and 240 min of PF-FeOx treatment.

In contrast, the MIC of MSSA 133 CipR was affected by *hv* and *hv*/H_2O_2, increasing and decreasing, respectively. Nonetheless, PF-Fe^{2+} and PF-FeOx did not modify their susceptibility. Since the changes in MIC were small and the alterations observed between the two MSSA were not consistent (even though they exhibited the same mechanism of resistance), these alterations post-treatment could be attributed to the margin of error in the measurement of MIC with ETEST® strips. However, VISA strains were consistently altered, and the MIC was increased by *hv* treatment, whereas it was decreased by PF-Fe^{2+} in both the strains. *The hv*/H_2O_2 and PF-FeOx treatments did not significantly affect the susceptibility of the strains.

3.4. Assessment of ARG degradation

For further application of PF processes in (waste)water treatment processes and to mitigate the risks of ARG spread, it is important to determine the differences in the efficiencies of the treatments for the degradation of ARG in the treated bacteria.

The β-lactam-resistant *E. coli* ESBL 8543, which contains $bla_{CTX\text{-}M\text{-}9}$ ARG [21], was treated with *hv*, *hv*/H_2O_2, PF-Fe^{2+}, and PF-FeOx. In the same study, it was established that the resistant strain was inactivated at the same rate as the susceptible strain for both the *hv* and PF-Fe^{2+} processes (5-log reduction was attained after 240 and 90 min of treatment, respectively). In addition, as there is no evidence that H_2O_2 does not diffuse into the ABR bacterial cell, causing the intracellular PF process, this strain is an adequate model for the present comparison with previously tested *S. aureus* strains under these conditions and treatment methods.

Fig. 3 shows the degradation of $bla_{CTX\text{-}M\text{-}9}$ after 300 min of *hv* treatment (lanes 5 to 9), 90 min of PF-Fe^{2+} treatment (lanes 14 to 18), 240 min of *hv*/H_2O_2 treatment (lanes 2 to 7), and 240 min of PF-FeOx treatment (lanes 11 to 17). It is clear that solar light alone cannot eliminate ARG completely, even if the quantity decreases consistently over time, despite the lack of DNA-mutating UVC irradiation. In fact, UVA-mediated intracellular oxidative events are able to completely inactivate bacteria within 300 min of treatment but do not completely degrade ARG. In contrast, PF-Fe^{2+} ensured the simultaneous complete inactivation of ARG and bacteria within 90 min of treatment.

Interestingly, PF-FeOx was faster than *hv*/H_2O_2 in *S. aureus* strains to achieve total inactivation, but its dependence on H_2O_2 concentration in the matrix and the diffusion gradient into the cell [57] and the slow reaction rate of the (extracellular) heterogeneous PF process [58] in *E. coli* resulted in concomitant gene elimination (similar levels after 240 min), while achieving cell wall destruction as an additional pathway for inactivation compared to *hv*/H_2O_2.

4. Discussion

With the rising concern of antibiotic resistance, new-generation antibiotics are currently the last-resort solutions for bacterial infection-related diseases. However, they are expected to gradually lose their effectiveness along with the acquisition of novel resistance mechanisms among bacteria. Several AOPs have been proposed as potential interventions to curb the spread of antibiotic resistance elements via WW disposal [12,59]. However, there are currently limited results on the use of photo-Fenton processes on ARB and ARG, especially detailing their modes of action.

The present study used *S. aureus* as a model bacterium because of its sanitary relevance and prevalence in the development of resistance to last-resort antibiotics such as ciprofloxacin and vancomycin. In fact, *S. aureus* was identified to develop mechanisms for CIP and VAN, which are the intracellular alteration of the binding site on the target enzyme and the extracellular alteration of the targeted sequence of amino acid residues, the expression of false target binding sites, and thickening of the cell wall, respectively.

As it is now well established that PF is effective for the disinfection of waterborne bacteria at acidic to near-neutral pH, we postulated that it could be applied for the effective inactivation of ARB and degradation of ARG under the conditions to elucidate the aforementioned propositions.

4.1. Does bacterial resistance to antibiotics necessarily mean resistance to advanced oxidation processes?

It is worth mentioning that the baseline damage from simulated solar light inactivated both resistant strains at the same rate as the susceptible strains, except for VISA 1050, which had a longer lag phase, before a sharper decrease, yielding a similar 4-log inactivation of 170 min (for both susceptible and resistant strains). For the strains with the intracellular mechanism of ABR, this is unsurprising, as the mechanism was shown to reside in the variation of an enzyme, and the sensitivity to light-induced oxidative stress through the internal PF process would not be altered. The slower effect of solar light on the external mechanism of resistance can be explained by (i) the favored formation of capsules protecting the bacteria, which has been extensively documented in vancomycin-resistant MRSA strains [60–62], and (ii) alteration of the cell wall peptidoglycan composition and arrangement, such as an increase in alcohol groups on muropeptides [53], alteration of terminal amino acids [63,64], and favoring an overall positive cell surface charge [65]. These changes may alter the absorption spectrum of the cell wall, especially in the UV region [66], which would attenuate the inhibition of enzymes related to the scavenging of intracellular H_2O_2 and $O_2^{\bullet-}$ thereby slowing down the intracellular Fenton process. Additionally, the acquisition of resistance to methicillin was linked to the lower expression of porphyrin [67]; thus, a reduction in its sensitivity to the bactericidal effect of light as an endogenous porphyrin acts as a photosensitizer [68].

In addition, the CIP-resistant strains did not show enhanced resistance to PF-Fe^{2+}, and their inactivation was identical to that of the susceptible strains. However, the rapid initial inactivation rate of VISA PC-3 * could be attributed to the lower production of staphyloxanthin, which was observed in certain MRSA strains after acquisition of resistance to VAN [65]. This antioxidant has been shown to effectively protects MRSA against oxidative stress, and its downregulation increases bacterial sensitivity to reactive oxygen species (ROS) [69]. This assumption is in accordance with the fact that the same initial rate is observed for the other two processes. For the same strain, the tailing effect was attributed to the formation of multicellular aggregates, as previously reported for this strain in the presence of VAN [31]; probably, the oxidative stress applied inflicts a similar type of response. Concerning VISA 1050, the slower inactivation by PF-Fe^{2+} was attributed to the simultaneous effect of the decreased diffusion of Fenton reagents because of the thicker cell wall and the attenuated effect of direct simulated sunlight. These effects would slow the intracellular Fenton effect and thus slow the overall inactivation rate.

Our results are consistent with those of previous studies. Typically, visible light inactivates MRSA and MSSA at the same [70] or quasi-identical rate [71]. These results are consistent in natural waters for vancomycin-resistant *Enterococcus* (VRE), β-lactam-producing *E. coli* (ESBL *E. coli*), and MRSA [72]. For disinfection with TiO_2, the acquisition of resistance to methicillin did not alter its susceptibility to the process, but the acquisition of VAN resistance significantly delayed the complete inactivation of *Enterococcus* [73]. Ozonation has also been extensively studied by comparing AB susceptibility to that of resistant strains. For instance, no resistance to ozonation has been observed in ABR strains of *E. coli*, *Enterococcus*, and *Staphylococcus* [74,75], except for VRE, whose inactivation rate nearly tripled [76]. Finally, through a UV-C/HSO_5^- process, similar inactivation of *E. coli*, *Enterococcus spp.*, *Pseudomonas spp.*, and their ARB counterparts has been achieved [77].

In conclusion, we suggest that the acquisition of internal or external mechanisms of resistance to antibiotics does not necessarily imply resistance to solar light-based processes, including homogeneous photo-Fenton processes, but may affect the inactivation rates of certain strains.

4.2. Does the AB resistance mechanism (internal/external) modify the bacterial susceptibility to the variants of the photo-Fenton process?

As mentioned previously, CIP-resistant strains were inactivated at the same pace when comparing PF-Fe^{2+} to PF-FeOx. However, it is interesting to mention that *hv*/H_2O_2 yielded the same inactivation in both PF processes for the MSSA 133 strain, whereas it was slightly slower for MSSA 1112. This suggests that inactivation of MSSA 133 is dominated by the intracellular Fenton reaction, whereas extracellular attacks play a significant role in MSSA 1112. However, as VISA 1050 was inactivated faster by PF-FeOx than by PF-Fe^{2+} and *hv*/H_2O_2, this suggests that the inactivation of this strain is dominated by extracellular bacterial damage, as the diffusion of Fenton reagents is limited by alteration of the cell wall. In the case of VISA PC-3 * , the initial rapid rate was dictated by the internal Fenton reaction, governed by intracellular hydrogen peroxide diffusion, since all three processes had the same initial rate. Past the point of rapid decrease, the expected formation of agglomerates slows inactivation by approximately 45 min. PF-FeOx becomes slower than PF-Fe^{2+} as the reduction of the available contact surface is greatly reduced and *hv*/H_2O_2 is the slowest, confirming that extracellular damage remains the main governing factor once aggregates are formed.

Here, some differences are worth mentioning and are explained based on the varied mechanisms of inactivation between the photo-Fenton processes applied. Nevertheless, we highlight that all treatments were faster than solar disinfection.

Variations were observed between the resistant and susceptible strains. However, several resistance mechanisms have not yet been assessed. Concerns may arise when applying the photo-Fenton process, especially regarding the mechanism of resistance related to the reduction of AB diffusion into the bacterial cell through the downregulation of porins. In fact, a porin-deficient mutant of AB-susceptible *E. coli* was shown to be less sensitive to the photo-Fenton process [78]. Although, to the best of our knowledge, there is no literature on the effect of PF on this type of resistance, the link between AB resistance and reduction of intracellular ferrous iron build-up is well-documented [79]. Provisionally, we suggest that the possibility that some ARB strains hinder Fenton reagent influx, causing variations between resistant and susceptible strains, cannot be excluded.

4.3. Is the threshold of antibiotic tolerance altered post-PF treatment?

Although it seems that solar light does not alter the MIC of strains with intracellular resistance mechanisms, it does increase the threshold of strains with extracellular resistance mechanisms. This may be due to the slower inactivation of these strains by solar light and a possible response to oxidative stress.

The *hv*/H_2O_2 test did not alter the MIC of either the external or internal ABR strains. This was also observed for the PF-FeOx treatment. This similarity is not surprising, as the intracellular effects of both treatments were similar, and PF-FeOx induced additional extracellular damage, which would not alter the ARG. This implies that the internal Fenton pathways resulting from the simultaneous effect of H_2O_2 diffusion and solar light are not sufficiently strong to trigger a reduction in resistance by gene (DNA) damage.

In contrast, PF-Fe^{2+} effectively reduced the MIC of the external ABR strains, although it did not alter the MICs of the intracellular ABR strains. This could be explained by the fact that *vanA*, a typical ARG related to VAN resistance, was identified to be located on plasmids [80], and the rapid inactivation induced by the combined intracellular and extracellular action of PF-Fe^{2+} may damage the location where resistance is expressed without compromising overall cell viability. This was corroborated by the PCR tests performed in the ESBL-producing strain, where the gene band disappeared in 15 min, but a high number of cultivable cells could be measured (see 4.4 for more details).

Overall, in the case of the tested ABR strains, it appeared that the enhancement of solar light with Fenton reagents led to faster inactivation and a reduction in the MIC post-treatment. This highlights a double gain, considering that, at the same time, the treatment time would be reduced and, in the contingency of bacterial regrowth, resistance to AB would be restricted. Additionally, this corroborates a previous study that achieved similar results with ceftazidime-resistant strains of *E. coli* and *Klebsiella pneumoniae* strains, which showed that their MIC decreased with PF-Fe^{2+} treatment [21]. To the best of our knowledge, these are the only examples of such investigations of post-treatment variation of MIC upon a (photo-)Fenton process, and we would suggest considering these results to be encouraging.

However, we would like to stress the need to be cautious about these conclusions, as other light-based and/or oxidative processes have yielded different results. For instance, treatment of two MDR *E. coli* strains (resistant to CIP, sulfamethoxazole, and amoxicillin) with UVC and chlorination generally left their MIC unchanged, as only one of the two strains was resistant to CIP, which was reduced by UVC light alone [81]. Another study reported that the use of TiO_2 as a photocatalyst increased the MIC of CIP, VAN, tetracycline, and cefuroxime in an MDR *E. coli* strain [82]. Finally, when comparing the evolution of resistance of a *K. pneumoniae* strain, another study detailed disinfection under UV, chlorination, and TiO_2 treatment [83]. They reported an increase in resistance to ampicillin and cefaclor under all treatments, a decrease in resistance towards tetracycline under all treatments, and an unchanged resistance towards sulfamethoxazole. Although the shift in resistance seems to be more dependent on the type of antibiotic resistance, TiO_2, which has an extracellular mode of action, tends to either increase or leave the resistance unchanged.

4.4. Does the mode of action of the photo-Fenton process (internal/external) induce different ARG degradation?

It is important to assess the potential spread of ARG that may occur post-AOP, especially considering that the PF-Fe^{2+} process alters the MIC of ARB with external mechanisms and not internal mechanisms.

It has been long shown that even after inactivation of ARB, the release of intracellular genes can perpetuate resistance through transformation by susceptible recipients [11]. Moreover, this phenomenon could be accelerated by the exposure of the recipient to ROS [84]. By monitoring the degradation of the ARG $bla_{CTX\text{-}M\text{-}9}$ in all four treatments, distinct patterns were observed. First, it is especially interesting to mention that a significant amount of ARG was degraded within 300 min of solar light treatment. On the other hand, a recent study [85] did not achieve a noticeable reduction in both extra- and intracellular ARG over a 60-minutes treatment under simulated solar irradiation, and no degradation of extracellular ARG under irradiation within the wavelength of 290–400 nm (UVB+UVA), but significant degradation at a wavelength of 254 nm (UVC) has been reported elsewhere [86]. Because the sun simulator used in this study has a cut-off of 290 nm (Figure S1) to comply with the received spectrum at the Earth's surface, this suggests that the intracellular Fenton pathways induced by solar light are sufficient for the degradation of genes. The *hv*-, *hv*/H_2O_2-, and PF-FeOx-mediated degradation of ARG was faster but not complete, confirming that the intracellular Fenton pathways, enhanced by the diffusion of hydrogen peroxide, were sufficient to enhance their destruction compared to solar light only, but not for complete degradation.

Finally, as PF-Fe^{2+} degraded a significant portion of the gene within 15 min, this confirmed that the homogeneous photo-Fenton process remained the most effective treatment for intracellular oxidative damage. However, it did not reduce MIC, suggesting that the genes conferring VAN and ESBL were degraded with different kinetics. This requires further investigation; however, provisionally, considering that each nucleotide has a different reactivity with $HO^{\bullet}$, we propose that their degradation might be linked to the gene composition of the bases and gene length [87,88].

5. Conclusions

This study assessed the hypothesis of possible interference of AR mechanisms with photo-Fenton process variants and constituents. The following conclusions can be drawn from the results:

- Solar light and heterogeneous photo-Fenton treatment inactivated antibiotic-resistant and antibiotic-sensitive strains, respectively, within the same timeframe.
- The mechanism of resistance to antibiotics may affect (i.e., increase) the sensitivity to the type of Fenton process.
- Both photo-Fenton types either remained unaltered or reduced the MIC; however, solar disinfection raised tolerance in some cases.
- Only homogeneous photo-Fenton treatment effectively reduced the concentration of $bla_{CTX\text{-}M\text{-}9}$ ARG.

These results reinforce the notion that antibiotic-resistant bacteria should not be considered special microorganisms during the application of the photo-Fenton process, but that genes are the main source of concern. Hence, the design of the treatment setup should instead aim to maximize the degradation of ARG, as genes were shown to be degraded at slower rates than bacterial inactivation, and ARB would already be inactivated. Finally, extrapolating this study to the general applications of the solar photo-Fenton process, we propose that an effective tertiary/quaternary treatment by the photo-Fenton process can result in safer discharge, recovery, and reuse of water resources with lower ARB/ARG risks.

CRediT authorship contribution statement

del Castillo Gonzalez Isabel: Writing – review & editing, Validation. **Entenza Jose Manuel:** Writing – original draft, Supervision, Methodology, Funding acquisition, Conceptualization. **Le Truong-Thien Melvin:** Writing – original draft, Investigation. **Decker Jeremie:** Writing – review & editing, Writing – original draft, Visualization, Investigation, Formal analysis. **Giannakis Stefanos:** Writing – review & editing, Writing – original draft, Validation, Supervision, Methodology, Investigation, Conceptualization. **Rodriguez-Chueca Jorge:** Writing – review & editing, Validation, Project administration. **Pulgarin Cesar:** Writing – review & editing, Supervision, Resources, Project administration, Methodology, Funding acquisition, Conceptualization. **Hernandez Lehmann Aurelio:** Writing – review & editing, Validation.

Declaration of Competing Interest

The authors declare that they have no known competing financial interests or personal relationships that could have appeared to influence the work reported in this paper.

Data Availability

Data will be made available on request.

Acknowledgements

Jeremie Decker, Stefanos Giannakis, and Jorge Rodriguez-Chueca would like to acknowledge the ARPHILAKE project, “Combating Antibiotic Resistance in Philippine Lakes: One Health upstream interventions to reduce the burden”, which received funding from the Agencia Estatal de Investigación (Spain), Proyectos de Colaboración Internacional (PCI2022-132918), under the umbrella of the “JPIAMR - Joint Programming Initiative on Antimicrobial Resistance.” Stefanos Giannakis would also like to acknowledge the DETRAS Project, “Desinfección-Descontaminación de Efluentes Contra la Transmisión de la Resistencia en Antibióticos” (APOYO-JOVENES-21-UXUKHL-88-WQWWQF), funded by the Comunidad de Madrid through the call “Research Grants for Young Investigators from Universidad Politécnica de Madrid”. Last, we would like to pay our gratitude and our respects to our deceased colleague, Dr. Josè Manuel Entenza-Pousada, for his collaboration, insights and fruitful scientific exchanges while hosting Truong-Thien Melvin Le at his laboratory, at the Department of Fundamental Microbiology of the University of Lausanne, Switzerland. A dedicated professor with a passion for research that will be remembered for his intellectual capacity, as well as his human qualities. He was in our thoughts through finalizing the manuscript, which we dedicate to honoring his memory.

Appendix A. Supporting information

Supplementary data associated with this article can be found in the online version at doi:10.1016/j.jece.2024.112147.

References

[1] W.A. Adedeji, The treasure called antibiotics, Ann. Ib. Post. Med 14 (2016) 56–57.
[2] IACG on Antimicrobial Resistance, No time to wait: Securing the future from drug-resistant infections, (2021). ⟨https://reliefweb.int/report/world/no-time-wait-securing-future-drug-resistant-infections-report-secretary-general-united⟩ (accessed March 14, 2023).
[3] U. Theuretzbacher, Global antibacterial resistance: the never-ending story, J. Glob. Antimicrob. Resist. 1 (2013) 63–69, https://doi.org/10.1016/j.jgar.2013.03.010.
[4] A. Karkman, T.T. Do, F. Walsh, M.P.J. Virta, Antibiotic-resistance genes in waste water, Trends Microbiol. 26 (2018) 220–228, https://doi.org/10.1016/j.tim.2017.09.005.
[5] D.M.P. De Oliveira, B.M. Forde, T.J. Kidd, P.N.A. Harris, M.A. Schembri, S. A. Beatson, D.L. Paterson, M.J. Walker, Antimicrobial Resistance in ESKAPE Pathogens, Clin. Microbiol Rev. 33 (2020) e00181-19, https://doi.org/10.1128/CMR.00181-19.
[6] J. O'Neill, Tackling drug-resistant infections globally: final report and recommendations, Government of the United Kingdom, 2016. ⟨https://apo.org.au/node/63983⟩ (accessed January 16, 2023).
[7] B. Aslam, M. Khurshid, M.I. Arshad, S. Muzammil, M. Rasool, N. Yasmeen, T. Shah, T.H. Chaudhry, M.H. Rasool, A. Shahid, X. Xueshan, Z. Baloch, Antibiotic resistance: one health one world outlook, Front Cell Infect. Microbiol 11 (2021) 771510, https://doi.org/10.3389/fcimb.2021.771510.
[8] L. Rizzo, C. Manaia, C. Merlin, T. Schwartz, C. Dagot, M.C. Ploy, I. Michael, D. Fatta-Kassinos, Urban wastewater treatment plants as hotspots for antibiotic resistant bacteria and genes spread into the environment: a review, Sci. Total Environ. 447 (2013) 345–360, https://doi.org/10.1016/j.scitotenv.2013.01.032.
[9] S. Giannakis, S. Rtimi, C. Pulgarin, Light-assisted advanced oxidation processes for the elimination of chemical and microbiological pollution of wastewaters in developed and developing countries, Molecules 22 (2017) 1070, https://doi.org/10.3390/molecules22071070.
[10] D.G.J. Larsson, C.-F. Flach, Antibiotic resistance in the environment, Nat. Rev. Microbiol 20 (2022) 257–269, https://doi.org/10.1038/s41579-021-00649-x.
[11] M.G. Lorenz, W. Wackernagel, Bacterial gene transfer by natural genetic transformation in the environment, Microbiol Rev. 58 (1994) 563–602.
[12] I. Michael-Kordatou, P. Karaolia, D. Fatta-Kassinos, The role of operating parameters and oxidative damage mechanisms of advanced chemical oxidation processes in the combat against antibiotic-resistant bacteria and resistance genes present in urban wastewater, Water Res. 129 (2018) 208–230, https://doi.org/10.1016/j.watres.2017.10.007.
[13] E. Ortega-Gómez, P. Fernández-Ibáñez, M.M. Ballesteros Martín, M.I. Polo-López, B. Esteban García, J.A. Sánchez Pérez, Water disinfection using photo-Fenton: Effect of temperature on Enterococcus faecalis survival, Water Res. 46 (2012) 6154–6162, https://doi.org/10.1016/j.watres.2012.09.007.
[14] J. Rodríguez-Chueca, M.I. Polo-López, R. Mosteo, M.P. Ormad, P. Fernández-Ibáñez, Disinfection of real and simulated urban wastewater effluents using a mild solar photo-Fenton, Appl. Catal. B: Environ. 150–151 (2014) 619–629, https://doi.org/10.1016/j.apcatb.2013.12.027.
[15] D. Rubio, E. Nebot, J.F. Casanueva, C. Pulgarin, Comparative effect of simulated solar light, UV, UV/H2O2 and photo-Fenton treatment (UV–Vis/H2O2/Fe2+,3+) in the Escherichia coli inactivation in artificial seawater, Water Res. 47 (2013) 6367–6379, https://doi.org/10.1016/j.watres.2013.08.006.
[16] E. Gualda-Alonso, N. Pichel, P. Soriano-Molina, E. Olivares-Ligero, F.X. Cadena-Aponte, A. Agüera, J.A. Sánchez Pérez, J.L. Casas López, Continuous solar photo-Fenton for wastewater reclamation in operational environment at demonstration scale, J. Hazard. Mater. 459 (2023) 132101, https://doi.org/10.1016/j.jhazmat.2023.132101.
[17] I. Arslan Alaton, A. Yazgan Karataş, Ö. Pehlivan, T. Olmez Hanci, Elimination of antibiotic resistance in treated urban wastewater by iron-based advanced oxidation processes, DWT 172 (2019) 235–253, https://doi.org/10.5004/dwt.2019.24929.
[18] I. Arslan-Alaton, A. Karatas, Ö. Pehlivan, O. Koba Ucun, T. Ölmez-Hancı, Effect of UV-A-assisted iron-based and UV-C-driven oxidation processes on organic matter and antibiotic resistance removal in tertiary treated urban wastewater, Catal. Today 361 (2021) 152–158, https://doi.org/10.1016/j.cattod.2020.02.037.

[19] G. Crini, E. Lichtfouse, Advantages and disadvantages of techniques used for wastewater treatment, Environ. Chem. Lett. 17 (2019) 145–155, https://doi.org/10.1007/s10311-018-0785-9.
[20] G. Maniakova, I. Salmerón, M. Aliste, M. Inmaculada Polo-López, I. Oller, S. Malato, L. Rizzo, Solar photo-Fenton at circumneutral pH using Fe(III)-EDDS compared to ozonation for tertiary treatment of urban wastewater: contaminants of emerging concern removal and toxicity assessment, Chem. Eng. J. 431 (2022) 133474, https://doi.org/10.1016/j.cej.2021.133474.
[21] S. Giannakis, T.-T.M. Le, J.M. Entenza, C. Pulgarin, Solar photo-Fenton disinfection of 11 antibiotic-resistant bacteria (ARB) and elimination of representative AR genes. Evidence that antibiotic resistance does not imply resistance to oxidative treatment, Water Res. 143 (2018) 334–345, https://doi.org/10.1016/j.watres.2018.06.062.
[22] S. Giannakis, S. Watts, S. Rtimi, C. Pulgarin, Solar light and the photo-Fenton process against antibiotic resistant bacteria in wastewater: a kinetic study with a Streptomycin-resistant strain, Catal. Today 313 (2018) 86–93, https://doi.org/10.1016/j.cattod.2017.10.033.
[23] I. De la Obra Jiménez, J.L.C. López, G.R. Ibáñez, B.E. García, J.A.S. Pérez, Kinetic assessment of antibiotic resistant bacteria inactivation by solar photo-Fenton in batch and continuous flow mode for wastewater reuse, Water Res. 159 (2019) 184–191, https://doi.org/10.1016/j.watres.2019.04.059.
[24] Y. Ahmed, J. Zhong, Z. Yuan, J. Guo, Simultaneous removal of antibiotic resistant bacteria, antibiotic resistance genes, and micropollutants by a modified photo-Fenton process, Water Res. 197 (2021) 117075, https://doi.org/10.1016/j.watres.2021.117075.
[25] Y. Ahmed, J. Lu, Z. Yuan, P.L. Bond, J. Guo, Efficient inactivation of antibiotic resistant bacteria and antibiotic resistance genes by photo-Fenton process under visible LED light and neutral pH, Water Res. 179 (2020) 115878, https://doi.org/10.1016/j.watres.2020.115878.
[26] G. Subramanian, H. Prakash, Photo augmented copper-based fenton disinfection under visible LED light and natural sunlight irradiation, Water Res. 190 (2021) 116719, https://doi.org/10.1016/j.watres.2020.116719.
[27] S. Giannakis, M.I. Polo López, D. Spuhler, J.A. Sánchez Pérez, P. Fernández Ibáñez, C. Pulgarin, Solar disinfection is an augmentable, in situ -generated photo-Fenton reaction—part 1: a review of the mechanisms and the fundamental aspects of the process, Appl. Catal. B: Environ. 199 (2016) 199–223, https://doi.org/10.1016/j.apcatb.2016.06.009.
[28] D. Spuhler, J. Andrés Rengifo-Herrera, C. Pulgarin, The effect of Fe2+, Fe3+, H2O2 and the photo-Fenton reagent at near neutral pH on the solar disinfection (SODIS) at low temperatures of water containing Escherichia coli K12, Appl. Catal. B: Environ. 96 (2010) 126–141, https://doi.org/10.1016/j.apcatb.2010.02.010.
[29] I. de la Obra Jiménez, S. Giannakis, D. Grandjean, F. Breider, G. Grunauer, J. L. Casas López, J.A. Sánchez Pérez, C. Pulgarin, Unfolding the action mode of light and homogeneous vs. heterogeneous photo-Fenton in bacteria disinfection and concurrent elimination of micropollutants in urban wastewater, mediated by iron oxides in Raceway Pond Reactors, Appl. Catal. B: Environ. 263 (2020) 118158, https://doi.org/10.1016/j.apcatb.2019.118158.
[30] P. Villegas- Guzman, S. Giannakis, S. Rtimi, D. Grandjean, M. Bensimon, L.F.L.F. De Alencastro, R. Torres-Palma, C. Pulgarin, A green solar photo-Fenton process for the elimination of bacteria and micropollutants in municipal wastewater treatment using mineral iron and natural organic acids, Appl. Catal. B: Environ. 219 (2017) 538–549, https://doi.org/10.1016/j.apcatb.2017.07.066.
[31] K. Sieradzki, R.B. Roberts, S.W. Haber, A. Tomasz, The development of vancomycin resistance in a patient with methicillin-resistant staphylococcus aureus infection, N. Engl. J. Med 340 (1999) 517–523, https://doi.org/10.1056/NEJM199902183400704.
[32] J.M. Entenza, J. Vouillamoz, M.P. Glauser, P. Moreillon, Levofloxacin versus ciprofloxacin, flucloxacillin, or vancomycin for treatment of experimental endocarditis due to methicillin-susceptible or -resistant Staphylococcus aureus, Antimicrob. Agents Chemother. 41 (1997) 1662–1667, https://doi.org/10.1128/AAC.41.8.1662.
[33] A. Dalhoff, Comparative in vitro and in vivo activity of the C-8 methoxy quinolone moxifloxacin and the C-8 chlorine quinolone BAY y 3118, Clin. Infect. Dis. 32 (2001) S16–S22, https://doi.org/10.1086/319371.
[34] M. Döring, English Wikipedia - Species Pages, (2022). https://doi.org/10.15468/C3KKGH.
[35] M.K.S. Ballo, S. Rtimi, S. Mancini, J. Kiwi, C. Pulgarin, J.M. Entenza, A. Bizzini, Bactericidal activity and mechanism of action of copper-sputtered flexible surfaces against multidrug-resistant pathogens, Appl. Microbiol Biotechnol. 100 (2016) 5945–5953, https://doi.org/10.1007/s00253-016-7450-7.
[36] R. Mosteo, A. Varon Lopez, D. Muzard, N. Benitez, S. Giannakis, C. Pulgarin, Visible light plays a significant role during bacterial inactivation by the photo-fenton process, even at sub-critical light intensities, Water Res. 174 (2020) 115636, https://doi.org/10.1016/j.watres.2020.115636.
[37] S. Samoili, G. Farinelli, J.Á. Moreno-SanSegundo, K.G. McGuigan, J. Marugán, C. Pulgarín, S. Giannakis, Predicting the bactericidal efficacy of solar disinfection (SODIS): from kinetic modeling of in vitro tests towards the in silico forecast of E. coli inactivation, Chem. Eng. J. 427 (2022) 130866, https://doi.org/10.1016/j.cej.2021.130866.
[38] J. Moreno-SanSegundo, S. Giannakis, S. Samoili, G. Farinelli, K.G. McGuigan, C. Pulgarín, J. Marugán, SODIS potential: A novel parameter to assess the suitability of solar water disinfection worldwide, Chem. Eng. J. 419 (2021) 129889, https://doi.org/10.1016/j.cej.2021.129889.
[39] A.H. Geeraerd, V.P. Valdramidis, J.F. Van Impe, GInaFiT, a freeware tool to assess non-log-linear microbial survivor curves, Int. J. Food Microbiol. 102 (2005) 95–105.
[40] A.H. Geeraerd, C.H. Herremans, J.F. Van Impe, Structural model requirements to describe microbial inactivation during a mild heat treatment, Int. J. Food Microbiol. 59 (2000) 185–209.
[41] S.-T. Han, Y. Fei, J.-Y. Huang, M. Xu, L.-C. Chen, D.J. Liao, Y.-J. Tan, Establishment of a simple and quick method for detecting extended-spectrum β-lactamase (ESBL) genes in bacteria, J. Biomol. Tech. 27 (2016) 132–137, https://doi.org/10.7171/jbt.16-2704-001.
[42] R. Davis, A. Markham, J.A. Balfour, Ciprofloxacin, Drugs 51 (1996) 1019–1074, https://doi.org/10.2165/00003495-199651060-00010.
[43] K. Drlica, X. Zhao, DNA gyrase, topoisomerase IV, and the 4-quinolones, Microbiol. Mol. Biol. Rev. 61 (1997) 377–392, https://doi.org/10.1128/mmbr.61.3.377-392.1997.
[44] L. Ferrero, B. Cameron, B. Manse, D. Lagneaux, J. Crouzet, A. Famechon, F. Blanche, Cloning and primary structure of Staphylococcus aureus DNA topoisomerase IV: a primary target of fluoroquinolones, Mol. Microbiol. 13 (1994) 641–653, https://doi.org/10.1111/j.1365-2958.1994.tb00458.x.
[45] M. Tanaka, T. Wang, Y. Onodera, Y. Uchida, K. Sato, Mechanism of quinolone resistance in Staphylococcus aureus, J. Infect. Chemother. 6 (2000) 131–139, https://doi.org/10.1007/s101560070010.
[46] D.P. Levine, Vancomycin: a history, Clin. Infect. Dis. 42 (2006) S5–S12, https://doi.org/10.1086/491709.
[47] R. Sobral, A. Tomasz, The staphylococcal cell wall, 7.4.12, Microbiol. Spectr. 7 (2019), https://doi.org/10.1128/microbiolspec.GPP3-0068-2019.
[48] P. Giesbrecht, T. Kersten, H. Maidhof, J. Wecke, Staphylococcal cell wall: morphogenesis and fatal variations in the presence of penicillin, Microbiol Mol. Biol. Rev. 62 (1998) 1371–1414, https://doi.org/10.1128/MMBR.62.4.1371-1414.1998.
[49] Hammes, Neuhaus, On the Mechanism of Action of Vancomycin: Inhibition of Peptidoglycan Synthesis in Gaffkya homari, (1974). https://doi.org/10.1128/AAC.6.6.722.
[50] N. Koyama, J. Inokoshi, H. Tomoda, Anti-infectious agents against MRSA, Molecules 18 (2013) 204–224, https://doi.org/10.3390/molecules18010204.
[51] L. Cui, X. Ma, K. Sato, K. Okuma, F.C. Tenover, E.M. Mamizuka, C.G. Gemmell, M.-N. Kim, M.-C. Ploy, N. El Solh, V. Ferraz, K. Hiramatsu, Cell wall thickening is a common feature of vancomycin resistance in staphylococcus aureus, J. Clin. Microbiol 41 (2003) 5–14, https://doi.org/10.1128/JCM.41.1.5-14.2003.
[52] P.M. Pereira, S.R. Filipe, A. Tomasz, M.G. Pinho, Fluorescence ratio imaging microscopy shows decreased access of vancomycin to cell wall synthetic sites in vancomycin-resistant staphylococcus aureus, Antimicrob. Agents Chemother. 51 (2007) 3627–3633, https://doi.org/10.1128/AAC.00431-07.
[53] H. Hanaki, K. Kuwahara-Arai, S. Boyle-Vavra, R.S. Daum, H. Labischinski, K. Hiramatsu, Activated cell-wall synthesis is associated with vancomycin resistance in methicillin-resistant Staphylococcus aureus clinical strains Mu3 and Mu50, J. Antimicrob. Chemother. 42 (1998) 199–209, https://doi.org/10.1093/jac/42.2.199.
[54] G. Li, M.J. Walker, D.M.P. De Oliveira, Vancomycin resistance in enterococcus and staphylococcus aureus, Microorganisms 11 (2022) 24, https://doi.org/10.3390/microorganisms11010024.
[55] G.-X. Huang, C.-Y. Wang, C.-W. Yang, P.-C. Guo, H.-Q. Yu, Degradation of bisphenol A by peroxymonosulfate catalytically activated with Mn1.8Fe1.2O4 nanospheres: synergism between Mn and Fe, ACS Publ. (2017), https://doi.org/10.1021/acs.est.7b03007.
[56] W.-Y. Pan, C.-C. Huang, T.-T. Lin, H.-Y. Hu, W.-C. Lin, M.-J. Li, H.-W. Sung, Synergistic antibacterial effects of localized heat and oxidative stress caused by hydroxyl radicals mediated by graphene/iron oxide-based nanocomposites, Nanomed.: Nanotechnol., Biol. Med. 12 (2016) 431–438, https://doi.org/10.1016/j.nano.2015.11.014.
[57] L. Feng, C. Peillex-Delphe, C. Lü, D. Wang, S. Giannakis, C. Pulgarin, Employing bacterial mutations for the elucidation of photo-Fenton disinfection: Focus on the intracellular and extracellular inactivation mechanisms induced by UVA and H2O2, Water Res. 182 (2020) 116049, https://doi.org/10.1016/j.watres.2020.116049.
[58] C. Ruales-Lonfat, J.F. Barona, A. Sienkiewicz, M. Bensimon, J. Vélez-Colmenares, N. Benítez, C. Pulgarín, Iron oxides semiconductors are efficients for solar water disinfection: a comparison with photo-Fenton processes at neutral pH, Appl. Catal. B: Environ. 166–167 (2015) 497–508, https://doi.org/10.1016/j.apcatb.2014.12.007.
[59] M.C.V.M. Starling, R.P. de Mendonça Neto, G.F.F. Pires, P.B. Vilela, C.C. Amorim, Combat of antimicrobial resistance in municipal wastewater treatment plant effluent via solar advanced oxidation processes: achievements and perspectives, Sci. Total Environ. 786 (2021) 147448, https://doi.org/10.1016/j.scitotenv.2021.147448.
[60] L. Cui, J.-Q. Lian, H. Neoh, E. Reyes, K. Hiramatsu, DNA microarray-based identification of genes associated with glycopeptide resistance in staphylococcus aureus, Antimicrob. Agents Chemother. 49 (2005) 3404–3413, https://doi.org/10.1128/AAC.49.8.3404-3413.2005.
[61] B.P. Howden, D.J. Smith, A. Mansell, P.D. Johnson, P.B. Ward, T.P. Stinear, J. K. Davies, Different bacterial gene expression patterns and attenuated host immune responses are associated with the evolution of low-level vancomycin resistance during persistent methicillin-resistant Staphylococcus aureus bacteraemia, BMC Microbiol 8 (2008) 39, https://doi.org/10.1186/1471-2180-8-39.
[62] F. McAleese, S.W. Wu, K. Sieradzki, P. Dunman, E. Murphy, S. Projan, A. Tomasz, Overexpression of genes of the cell wall stimulon in clinical isolates of staphylococcus aureus exhibiting vancomycin-intermediate- S. aureus-type resistance to vancomycin, J. Bacteriol. 188 (2006) 1120–1133, https://doi.org/10.1128/JB.188.3.1120-1133.2006.

[63] I.G. Boneca, N. Xu, D.A. Gage, B.L.M. de Jonge, A. Tomasz, Structural characterization of an abnormally cross-linked muropeptide dimer that is accumulated in the peptidoglycan of methicillin- and cefotaxime-resistant mutants of staphylococcus aureus, J. Biol. Chem. 272 (1997) 29053–29059, https://doi.org/10.1074/jbc.272.46.29053.
[64] B.L. de Jonge, Y.S. Chang, D. Gage, A. Tomasz, Peptidoglycan composition of a highly methicillin-resistant Staphylococcus aureus strain. The role of penicillin binding protein 2A, J. Biol. Chem. 267 (1992) 11248–11254, https://doi.org/10.1016/S0021-9258(19)49903-1.
[65] C. Vidaillac, S. Gardete, R. Tewhey, G. Sakoulas, G.W. Kaatz, W.E. Rose, A. Tomasz, M.J. Rybak, Alternative mutational pathways to intermediate resistance to vancomycin in methicillin-resistant Staphylococcus aureus, J. Infect. Dis. 208 (2013) 67–74, https://doi.org/10.1093/infdis/jit127.
[66] S. Prasad, I. Mandal, S. Singh, A. Paul, B. Mandal, R. Venkatramani, R. Swaminathan, Near UV-Visible electronic absorption originating from charged amino acids in a monomeric protein, Chem. Sci. 8 (2017) 5416–5433, https://doi.org/10.1039/C7SC00880E.
[67] A. Lipovsky, Y. Nitzan, H. Friedmann, R. Lubart, Sensitivity of *Staphylococcus aureus* strains to broadband visible light, Photochem. Photobiol. 85 (2009) 255–260, https://doi.org/10.1111/j.1751-1097.2008.00429.x.
[68] S. Giannakis, A. Gupta, C. Pulgarin, J. Imlay, Identifying the mediators of intracellular E. coli inactivation under UVA light: The (photo) Fenton process and singlet oxygen, Water Res. 221 (2022) 118740, https://doi.org/10.1016/j.watres.2022.118740.
[69] A. Valliammai, A. Selvaraj, P. Muthuramalingam, A. Priya, M. Ramesh, S. K. Pandian, Staphyloxanthin inhibitory potential of thymol impairs antioxidant fitness, enhances neutrophil mediated killing and alters membrane fluidity of methicillin resistant Staphylococcus aureus, Biomed. Pharm. 141 (2021) 111933, https://doi.org/10.1016/j.biopha.2021.111933.
[70] M. Maclean, S.J. MacGregor, J.G. Anderson, G. Woolsey, Inactivation of bacterial pathogens following exposure to light from a 405-nanometer light-emitting diode array, Appl. Environ. Microbiol 75 (2009) 1932–1937, https://doi.org/10.1128/AEM.01892-08.
[71] M. Maclean, S.J. MacGregor, J.G. Anderson, G. Woolsey, High-intensity narrow-spectrum light inactivation and wavelength sensitivity of *Staphylococcus aureus*, FEMS Microbiol. Lett. 285 (2008) 227–232, https://doi.org/10.1111/j.1574-6968.2008.01233.x.
[72] T. Azuma, T. Hayashi, Effects of natural sunlight on antimicrobial-resistant bacteria (AMRB) and antimicrobial-susceptible bacteria (AMSB) in wastewater and river water, Sci. Total Environ. 766 (2021) 142568, https://doi.org/10.1016/j.scitotenv.2020.142568.
[73] T.-M. Tsai, H.-H. Chang, K.-C. Chang, Y.-L. Liu, C.-C. Tseng, A comparative study of the bactericidal effect of photocatalytic oxidation by TiO2 on antibiotic-resistant and antibiotic-sensitive bacteria, J. Chem. Technol. Biotechnol. 85 (2010) 1642–1653, https://doi.org/10.1002/jctb.2476.
[74] S. Heß, C. Gallert, Sensitivity of antibiotic resistant and antibiotic susceptible Escherichia coli, Enterococcus and Staphylococcus strains against ozone, J. Water Health 13 (2015) 1020–1028, https://doi.org/10.2166/wh.2015.291.
[75] K. Kirchner, I. Brückner, K. Klaer, M. Hammers-Wirtz, J. Pinnekamp, M. A. Rosenbaum, Microbial counts and antibiotic resistances during conventional wastewater treatment and wastewater ozonation, Ozone.: Sci. Eng. 42 (2020) 108–119, https://doi.org/10.1080/01919512.2019.1645641.
[76] T. Azuma, T. Hayashi, Disinfection of antibiotic-resistant bacteria in sewage and hospital effluent by ozonation, Ozone.: Sci. Eng. 43 (2021) 413–426, https://doi.org/10.1080/01919512.2021.1906095.
[77] I. Berruti, S. Nahim-Granados, M.J. Abeledo-Lameiro, I. Oller, M.I. Polo-López, UV-C peroxymonosulfate activation for wastewater regeneration: simultaneous inactivation of pathogens and degradation of contaminants of emerging concern, Molecules 26 (2021) 4890, https://doi.org/10.3390/molecules26164890.
[78] S. Giannakis, M. Voumard, S. Rtimi, C. Pulgarin, Bacterial disinfection by the photo-Fenton process: extracellular oxidation or intracellular photo-catalysis? Appl. Catal. B: Environ. 227 (2018) 285–295, https://doi.org/10.1016/j.apcatb.2018.01.044.
[79] J.B. Brown, M.A. Lee, A.T. Smith, Ins and outs: recent advancements in membrane protein-mediated prokaryotic ferrous iron transport, Biochemistry 60 (2021) 3277–3291, https://doi.org/10.1021/acs.biochem.1c00586.
[80] L.M. Weigel, D.B. Clewell, S.R. Gill, N.C. Clark, L.K. McDougal, S.E. Flannagan, J. F. Kolonay, J. Shetty, G.E. Killgore, F.C. Tenover, Genetic analysis of a high-level vancomycin-resistant isolate of *Staphylococcus aureus*, Science 302 (2003) 1569–1571, https://doi.org/10.1126/science.1090956.
[81] A. Rizzo, A. Fiorentino, Anselmo, Advanced treatment of urban wastewater by UV radiation: effect on antibiotics and antibiotic-resistant E. coli strains, Chemosphere 92 (2013) 171–176, https://doi.org/10.1016/j.chemosphere.2013.03.021.
[82] L. Rizzo, D. Sannino, V. Vaiano, O. Sacco, A. Scarpa, D. Pietrogiacomi, Effect of solar simulated N-doped TiO2 photocatalysis on the inactivation and antibiotic resistance of an E. coli strain in biologically treated urban wastewater, Appl. Catal. B: Environ. 144 (2014) 369–378, https://doi.org/10.1016/j.apcatb.2013.07.033.
[83] D. Venieri, I. Gounaki, M. Bikouvaraki, V. Binas, A. Zachopoulos, G. Kiriakidis, D. Mantzavinos, Solar photocatalysis as disinfection technique: Inactivation of Klebsiella pneumoniae in sewage and investigation of changes in antibiotic resistance profile, J. Environ. Manag. 195 (2017) 140–147, https://doi.org/10.1016/j.jenvman.2016.06.009.
[84] H. Li, A. Dechesne, Z. He, M.M. Jensen, H.L. Song, B.F. Smets, Electrochemical disinfection may increase the spread of antibiotic resistance genes by promoting conjugal plasmid transfer, Sci. Total Environ. 858 (2023) 159846, https://doi.org/10.1016/j.scitotenv.2022.159846.
[85] L.T. Zhang, R. Xu, J.G. Liu, Special issue in honour of Prof. Reto J. Strasser – Efficacy of botanical pesticide for rotifer extermination during the cultivation of Nannochloropsis oculata probed by chlorophyll a fluorescence transient, Photosynthetica 58 (2020) 341–347, https://doi.org/10.32615/ps.2019.164.
[86] M. Nihemaiti, Y. Yoon, H. He, M.C. Dodd, J.-P. Croue, Y. Lee, Degradation and deactivation of a plasmid-encoded extracellular antibiotic resistance gene during separate and combined exposures to UV254 and radicals, Water Res. 11 (2020).
[87] H. He, P. Zhou, K.K. Shimabuku, X. Fang, S. Li, Y. Lee, M.C. Dodd, Degradation and deactivation of bacterial antibiotic resistance genes during exposure to free chlorine, monochloramine, chlorine dioxide, ozone, ultraviolet light, and hydroxyl radical, Environ. Sci. Technol. 53 (2019) 2013–2026, https://doi.org/10.1021/acs.est.8b04393.
[88] X. Liu, J.Y. Hu, Effect of DNA sizes and reactive oxygen species on degradation of sulphonamide resistance sul1 genes by combined UV/free chlorine processes, J. Hazard. Mater. 392 (2020) 122283, https://doi.org/10.1016/j.jhazmat.2020.122283.